Technology in Cancer Research & Treatment
Volume 18: 1-13

DOI: 10.1177/1533033819876307
journals.sagepub.com/home/tct
SAGE

A Study on Nonthermal Irreversible Electroporation of the Thyroid

Yanpeng Lv, PhD[1,2], Yanfang Zhang, MD, PhD*[,2,3], Jianwei Huang, MD[4], Yunlong Wang, PhD[5], and Boris Rubinsky, PhD[2]

Abstract

Background: Nonthermal irreversible electroporation is a minimally invasive surgery technology that employs high and brief electric fields to ablate undesirable tissues. Nonthermal irreversible electroporation can ablate only cells while preserving intact functional properties of the extracellular structures. Therefore, nonthermal irreversible electroporation can be used to ablate tissues safely near large blood vessels, the esophagus, or nerves. This suggests that it could be used for thyroid ablation abutting the esophagus. This study examines the feasibility of using nonthermal irreversible electroporation for thyroid ablation. **Methods:** Rats were used to evaluate the effects of nonthermal irreversible electroporation on the thyroid. The procedure entails the delivery of high electric field pulses (1-3 kV/cm, 100 microseconds) between 2 surface electrodes bracing the thyroid. The right lobe was treated with various nonthermal irreversible electroporation pulse sequences, and the left was the control. After 24 hours of the nonthermal irreversible electroporation treatment, the thyroid was examined with hemotoxylin and eosin histological analysis. Mathematical models of electric fields and the Joule heating-induced temperature raise in the thyroid were developed to examine the experimental results. **Results:** Treatment with nonthermal irreversible electroporation leads to follicular cells damage, associated with cell swelling, inflammatory cell infiltration, and cell ablation. Nonthermal irreversible electroporation spares the trachea structure. Unusually high electric fields, for these types of tissue, 3000 V/cm, are needed for thyroid ablation. The mathematical model suggests that this may be related to the heterogeneous structure of the thyroid-induced distortion of local electric fields. Moreover, most of the tissue does not experience thermal damage inducing temperature elevation. However, the heterogeneous structure of the thyroid may cause local hot spots with the potential for local thermal damage. **Conclusion:** Nonthermal irreversible electroporation with 3000 V/cm can be used for thyroid ablation. Possible applications are treatment of hyperthyroidism and thyroid cancer. The highly heterogeneous structure of the thyroid distorts the electric fields and temperature distribution in the thyroid must be considered when designing treatment protocols for this tissue type.

Keywords

thyroid, hyperthyroidism, nonthermal irreversible electroporation, minimally invasive surgery, thyroid cancer

Abbreviations

ATDs, antithyroid drugs; IRE, irreversible electroporation; H&E, hematoxylin and eosin; NTIRE, nonthermal irreversible electroporation.

Received: March 28, 2019; Revised: August 14, 2019; Accepted: August 23, 2019.

Introduction

The thyroid gland is an endocrine gland in the neck made of 2 lobes connected by an isthmus and bracing the larynx. The function of the thyroid is to produce, store, and secrete the iodine-based hormones tri-iodothyronine and thyroxine.[1] A cross-section in a normal rat thyroid tissue is shown in Figure 1A. The thyroid has an interesting structure. It is made of hormone secretory cells surrounding cavities filled with a colloid. The hormones generated by the secretary cells are stored in the colloidal cavity. The cavity and the surrounding

[1] School of Electrical Engineering, Zhengzhou University, Zhengzhou, China
[2] Department of Mechanical Engineering and Department of Bioengineering University of California, Berkeley, CA, USA
[3] Department of Endocrinology, Luoyang Central Hospital Affiliated to Zhengzhou University, Luoyang, China
[4] Department of Pathology, Luoyang Central Hospital Affiliated to Zhengzhou University, Luoyang, China
[5] Henan Bioengineering Research Center, Zhengzhou, China
*is the co-first author.

Corresponding Author:
Yanfang Zhang, PhD, Department of Endocrinology, Luoyang Central Hospital Affiliated to Zhengzhou University, Luoyang, China.
Email: xxzhangin@163.com

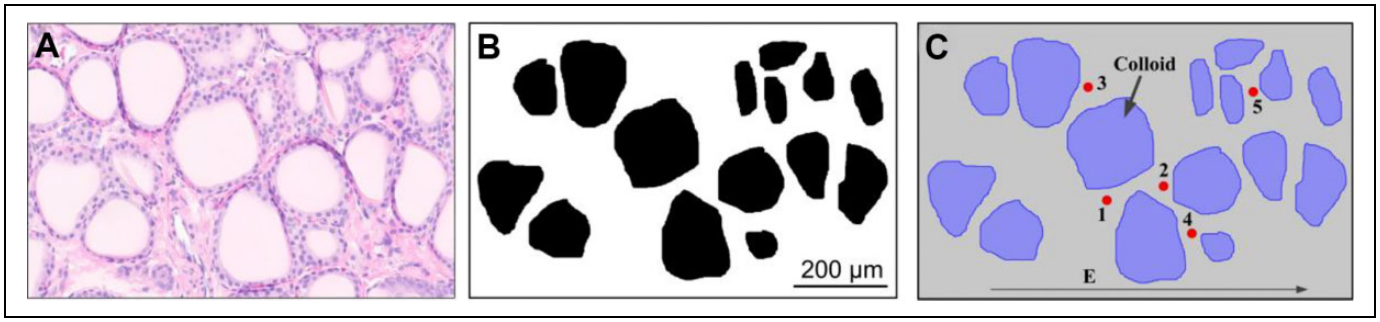

Figure 1. (A) H&E staining image of normal rat thyroid tissue. The figure shows the colloid cavity structures (the empty spaces are the colloidal cavity and the dark dots surrounding the cavity are the cells). (B) Grayscale image depicted in (A). (C) Model in COMSOL software. H&E indicates hematoxylin and eosin.

cells complex are known as a follicle.[2] The secretory cells release the hormones into this "cavity" where it is bound by a glycoprotein and stored as a "colloid." The follicular cells continuously generate the hormone, which is stored in the colloid cavity that grows in time as it incorporates the hormone. To secrete the hormone, the hormone is reabsorbed from the cavity and then released into the surrounding interstitial spaces.[3]

Hyperthyroidism is characterized by increased thyroid hormone synthesis and secretion from the thyroid gland. The elevated level of thyroid hormones can result in clinical manifestations ranging from mild to severe toxicity. Next to diabetes mellitus and osteoporosis, hyperthyroidism is one of the most common endocrine disorders[4]. Excess thyroid hormone affects many different organ systems. Commonly reported symptoms are palpitations, fatigue, anxiety, disturbed sleep, weight loss, heat intolerance, sweating, and polydipsia. Frequent physical findings are tachycardia, tremor of the extremities, and weight loss.[5,6] Approximately 3% of women and 0.5% of men will develop Graves' disease, the most common cause of persistent hyperthyroidism in adults.[7]

The 3 common options for treating patients with hyperthyroidism are antithyroid drugs (ATDs), radioactive iodine ablation, and surgery. Antithyroid drugs are a preferred primary treatment. Antithyroid drugs can control the clinical manifestation and reduce the thyroid hormone level to normal, in most patients. However, ATDs have side effects and drawbacks. The medication must be taken for between 12 and 18 months, which leads to difficulties with compliance.[8] Patients experience a high rate of relapse, between 50% and 55%.[9,10] The incidences of drug side effects, such as agranulocytosis, hepatotoxicity, and pruritus, have been estimated to be between 0.1% and 5%.[11,12] Radioactive iodine therapy is also a common treatment, especially in North America.[13] Radioactive iodine therapy is a safe and cost-effective choice. However, calculating the correct dosage is challenging, with miscalculations causing the outcome of the procedure to vary from hyperthyroidism to hypothyroidism. Furthermore, women in pregnancy, breast-feeding, and planning pregnancy are absolutely restricted from this therapy. Thyroidectomy is the third way of treating hyperthyroidism. It is recommended for patients having contraindications of ATDs or radioactive iodine.[14] The most frequent complication of thyroidectomy is hypocalcaemia due to permanent hypoparathyroidism and complications from surgery such as permanent recurrent laryngeal nerve injury.[15]

The goal of this study is to introduce and evaluate the feasibility of using a new minimally invasive surgical technology, nonthermal irreversible electroporation (NTIRE), for thyroid tissue ablation. Electroporation is the permeabilization of the cell membrane with microsecond-long, high electric field pulses delivered across a cell.[16,17] According to the magnitude of electric fields used, the permeabilization can be transient in a process known as reversible electroporation or permanent in a process known as irreversible electroporation (IRE). While reversible electroporation has become the gold standard for genetic engineering since first introduced for this purpose in 1982,[18] the value of IRE in minimally invasive surgery was recognized only recently. When delivered in a form that minimizes thermal damage, NTIRE electric pulses affect only the cell membrane and spare the extracellular matrix and sensitive structure within and around the treated area.[19-22] On the strength of its ablative selectivity, NTIRE has gained importance in clinical tissue ablation near sensitive structures such as near large lumen in the liver[23] and in the pancreas.[24] Recent studies have also shown that, unlike thermal ablation such as with radiofrequency and microwave, NTIRE can be safely used for tissue ablation near the esophagus, sparing the extracellular structure of the esophagus and nerves.[25-27] Electroporation involves inserting 2 or more thin needle electrodes to brace the targeted tissue or inserting one thin bipolar electrode in the targeted tissue, under ultrasound monitoring, and application of several microsecond-long electric pulses in a procedure that usually lasts less than a minute. It can also be done percutaneously. The finding that NTIRE can be safely used for tissue ablation near the esophagus, sparing the extracellular structure of the esophagus, and nerves[25-27] have led us to suggest and explore in this study the use of NTIRE as a simple technique for minimally invasive surgical ablation of the thyroid. The use of NTIRE may have advantages over other thyroid ablation techniques as it can be used repeatedly, since the procedure does not involve drugs or radioactive isotopes.

The potential use of NTIRE to treat hyperthyroidism was discussed earlier. In addition, NTIRE may be useful for treatment of thyroid cancer. Patients usually choose to have an invasive thyroidectomy (surgical removal of the thyroid). While the procedure has a high rate of success, if the entire thyroid is removed (total thyroidectomy), the patient requires daily treatment with thyroid hormone to replace the thyroid's natural function for the rest of their life. However, if only a portion is removed (partial thyroidectomy), the thyroid may be able to function normally after surgery.[28,29] Focal ablation is of growing interest in treatment of cancer. During the last 5 years, NTIRE has been already used for focal therapy to treat thousands of patients with liver cancer,[30] pancreas cancer,[31] and prostate cancer.[22] This minimally invasive surgery may also have value for treatment of the hyperthyroidism or thyroid cancer. The goal of this study is to evaluate the feasibility and to characterize the use of NTIRE for tissue ablation in the thyroid of a small animal model.

Materials and Methods

In Vivo *Experimental Procedure*

Eighteen Sprague-Dawley rats weighing 312 $\pm$ 71 g were used in this study. All animals received humane care from properly trained professionals in compliance with both the Principals of Laboratory Animal Care and the Guide for the Care and Use of Laboratory Animals, published by the National Institute of Health (NIH publication no 85-23, revised 1985).

Animals were anaesthetized with 2 mg/kg meloxicam and 0.05 mg/kg buprenorphine followed by chamber induction with isoflurane. Bupivacaine (up to 8 mg/kg) was administered subcutaneously along the midline of the abdomen as a local anesthesia. Anesthesia was administered throughout the procedure with vaporized isoflurane. The depth of anesthesia was assessed prior to surgery and during the surgery by monitoring the rats' reflexes to pressure on their tail and feet. The breathing rate and the color of the nose and tongue were also monitored and recorded. The depth of anesthesia was assessed before surgery and throughout the surgical procedure. After the level of anesthesia was verified, a midline skin incision is made along the length of the neck. The underlying tissues and salivary glands are retracted laterally. The thyroid muscle is separated from the lobes of the thyroid gland. The thyroid glands are exposed. Extreme care is taken not to damage the trachea and laryngeal nerve. Sterile surgical techniques were used throughout the entire surgery. The thyroid has 2 lobes; therefore, using 1 lobe as control excludes bias between individuals. The right lobe was treated in each animal, and the left lobe was used as control. After partial mobilization of the thyroid from adjacent tissue, the right thyroid lobe was gently clamped between 2 flat parallel 3-mm diameter platinum electrodes (Harvard Apparatus, Holliston, Massachusetts). The distance between the 2 plate electrodes was 1 mm and was consistent for all the animals tested. A sequence of 10 or 30 square pulse with voltage over distance of 1000 V/cm, 2000 V/cm, or 3000 V/cm, 100-microsecond pulse width, separated by 100 millisecond, was applied between the electrodes, across the thyroid, using a high-voltage pulse generator designed for electroporation procedures (ECM 830, Harvard Apparatus). At the end of the experiment, the skin was closed and sutured. Tissue adhesive and a stapler were applied over the skin sutures. The animals were given 2 additional doses of buprenorphine (0.05 mg/kg) and meloxicam (2 mg/kg), spaced out over 8-hour increments. Symptoms that were monitored included reduced food intake, fever, hunched posture, lack of grooming or locomotion, swelling around the incision, facial discharges around the nose and eye, and diarrhea. We examine the thyroid via thyroid harvest at 24 hours after treatment. As this is the first time NTIRE technology was applied in thyroid ablation, we choose the 24 hours as the end point time to evaluate thyroid ablation. The choice of this end point was motivated by the results of our experiments with liver ablation, where we found that the NTIRE-ablated hepatocytes regenerated within 24 hours.[32] Obviously, further studies are needed to explore the long-term dynamics of physiological events in thyroid tissue treated with NTIRE. Animals were euthanized by a combination of an overdose of vaporized isoflurane and a bilateral chest dissection.

Immunohistochemistry

The thyroid lobes were fixed with 10% neutral-buffered formalin and submitted to an independent pathology laboratory (Histo-Tec Laboratory, Hayward, California). The samples were embedded in paraffin and sectioned with a microtome (5-μ m thick). All samples were cut vertically to the long axis of thyroid lobe, in a plane that followed the direction from the positive to the negative electrode, thereby exposing the treated thyroid area cross-section. Hematoxylin and eosin (H&E) staining was used to examine the morphology of the treated thyroid lobe and the control.

Mathematical Model of Electric Field

Figure 1A shows an H&E staining image of normal rat thyroid tissue. The thyroid tissue is heterogeneous and consists of colloidal structures of various dimensions surrounded by thyroid cells. This image was used to study the effects of the heterogeneity on the electric fields that develop during electroporation. The image was imported into GIMP 2.10 (GNU Image Manipulation Program, freeware; http://www.gimp.com). The edges of 15 colloids were extracted to generate a grayscale image. The colloids were separated for easier segmentation (Figure 1B). The grayscale image was imported into MATLAB. The finite elements calculation was performed by COMSOL Multiphysics (COMSOL, Burlington, Massachusetts) with the aid of the MATLAB-coupled LiveLink interface (Figure 1C). The whole computational domain was modeled as a 1.1 mm length square. The distance between 2 electrodes was set to 1 mm as in the experiments (Figure 2). The voltages were applied to the all lines of left electrode. The right electrode was

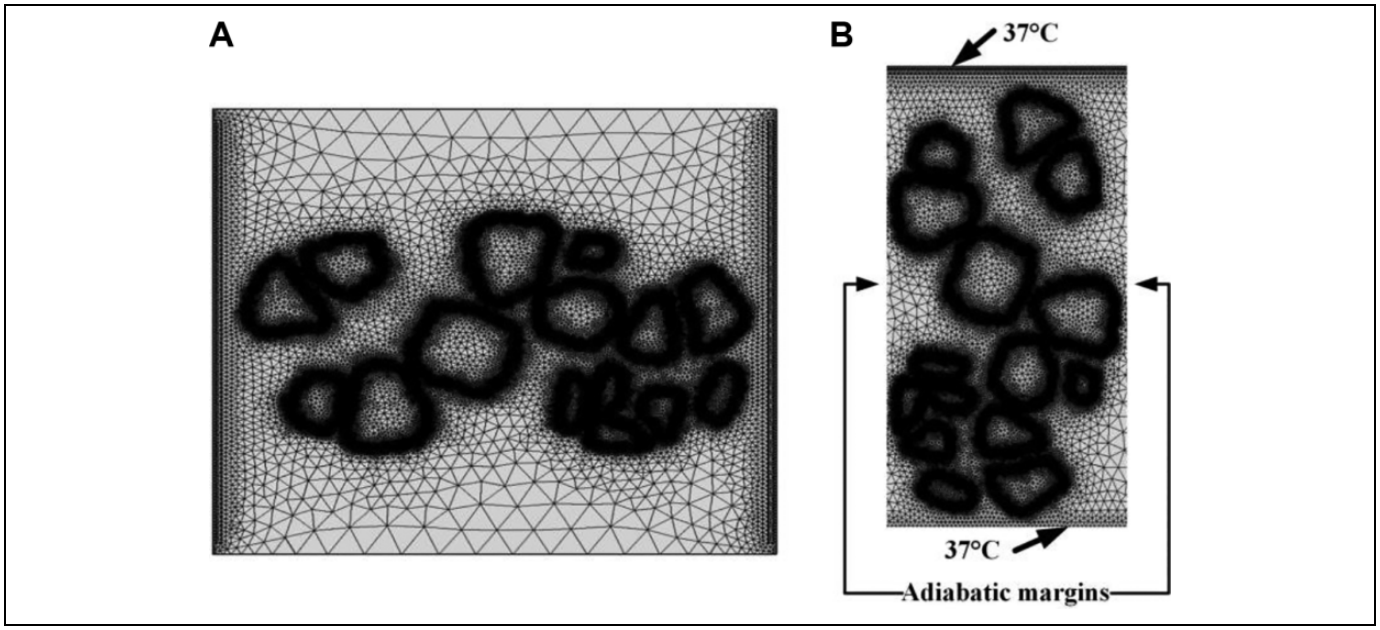

Figure 2. The finite element mesh used in the simulation. The geometry (B) analyzed for heat transfer is the heterogeneous excerpt from A.

taken to ground (0 V), and the left electrode was given a positive voltage. The thyroid is a highly heterogeneous tissue and the detailed electric and thermal properties of the thyroid are not available. Therefore, we used what we consider reasonable assumptions in populating the mathematical data with properties data. The conductivity of the electrodes was taken to be that of a metal of 5.998×10^6 S/m. Since the colloid is a type of gel, the conductivity of the colloid was set to that of a pure gel of 0.0529 S/m.[33] To better understand the effects of the electrical properties of the colloid on the electric field that develops during the electroporation of thyroid tissue, we also performed a parametric study using different values for the conductivity of the colloid (0.001, 0.01, 0.05, 0.1, 0.25, and 0.5 S/cm). The conductivity of the tissue surrounding the colloid was set to the average thyroid tissue conductivity of 0.511 S/m[34] (https://itis.swiss/virtual-population/tissue-properties/database/dielectric-properties/).

The Electric Currents module in COMSOL was used to solve computational domain with a free triangle mesh using the Normal preset values. All external line boundaries were set as insulators by the following equations:

$$n \bullet J = 0 \tag{1}$$

Electric potential V was calculated in the computational domain by the Laplace equation:

$$\nabla^2 V = 0 \tag{2}$$

The electric current density J distribution can be solved by the following equation:

$$\nabla \bullet J = Q \tag{3}$$

$$J = \sigma E + J_e \tag{4}$$

where J is the current density, Q is the electric charge, J_e is the external current.

The electric field E distribution can be calculated by the following equation:

$$E = -\nabla V \tag{5}$$

Figure 1C shows the 5 points near the colloidal inclusions which we used in the analysis of the results. These 5 points were chosen at random in the region between the colloids.

Mathematical Model of Temperature Distribution

A numerical simulation was performed to estimate the possibility of Joule heating induced thermal damage in the electroporation treated tissue. The numerical model simulates the treatment of a 2-dimensional heterogeneous thyroid tissue. The geometry analyzed for heat transfer is the heterogeneous excerpt from Figure 2A, shown in Figure 2B. As with the calculation of the electric fields, the thermal analysis is hampered by the fact that the thermal properties of the colloid and the tissue between the colloids in the thyroid are not known. Therefore, the thermal properties were chosen to be homogeneous at the bulk thermal properties' values of a thyroid. We assume that thermal properties are affected by heterogeneity less than electric properties. Obviously, all these assumptions lead to a first-order evaluation of the thermal history during the electroporation process, and future studies must try and develop models with more accurate data. Nevertheless, it will be shown later that even this highly simplified model also produces some interesting insight into the thermal characteristics of the process.

The analysis was performed using a thermal numerical model from Comsol Multiphysics 5.0, as described in the work of Daniels and Rubinsky[35]. Specifically, the electrical potential

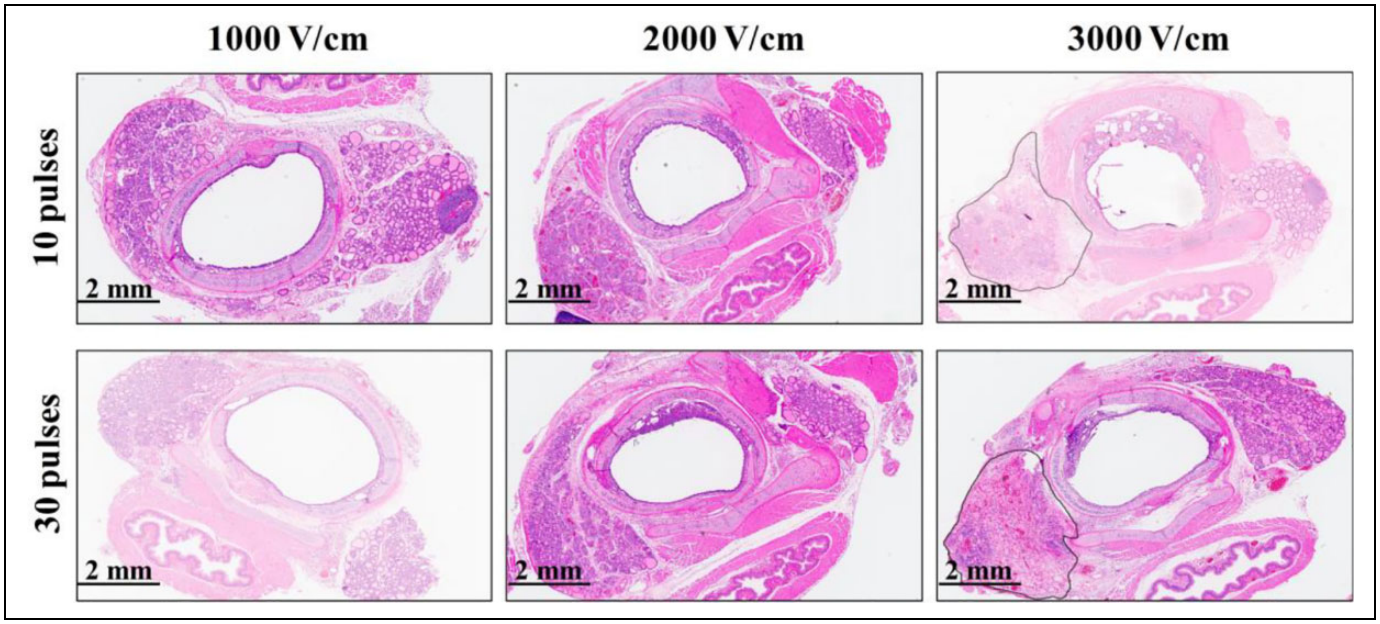

Figure 3. Macroscopic cross-section of the treated thyroid around the esophagus. Cross-section normal to the esophagus. The left side of the esophagus is the treated lobe, and the right side of the esophagus is the control. The images are shown as a function of electric voltage/distance between the electrodes and the number of pulses. Complete damage was observed only for 3000 V/cm and the damages are marked.

was calculated from Equations 1 to 5 and the temperature T in time t from an equation that ignores the effect of blood flow and therefore also gives an upper limit to the temperature:

$$\nabla(k\nabla T) + q'' = \rho c \frac{\partial T}{\partial t} \tag{6}$$

where k is the thermal conductivity, q'' is the electrical energy dissipated, c is the heat capacity, and ρ is the density. The model assumes that the initial temperature of the thyroid tissue is 37°C. The thermal conductivity, W/(m·K), heat capacity, J/(kg·K), and density, kg/m^3, of the thyroid were taken to be, 0.52, 3609, and 1050, respectively.

The analysis is complicated by the highly heterogeneous structure of the thyroid and the complex electric current distribution in the thyroid. The heat due to the electrical energy dissipation was calculated from the solution to Equations 1-5 using the expression:

$$q'' = \sigma|\nabla\phi|^2 \tag{7}$$

To provide the upper limit of the temperature distribution, we assumed that the electrodes are at 37°C, although it is more likely that they are at room temperature, 20°C. The edges of the heterogeneous slab are assumed adiabatic. Blood flow is also ignored. The initial temperature of the tissue is also assumed 37°C. These choices were made to generate an upper limit estimate for the temperature distribution in the treated thyroid tissue.

Results

Continuous monitoring of the animals indicated that the animals did not experience any adverse effects from the NTIRE treatment procedure. As indicated earlier, in this study, we compared the effects of the number of pulses and electric fields magnitude between electrodes on the histology of the thyroid, 24 hours after treatment. The parameters were, 10 and 30 pulses with electric fields of 1000 V/cm, 2000 V/cm, and 3000 V/cm; 100 microsecond; and 100-millisecond interval time (10 pulses per second). Current clinical applications of NTIRE use a pulse delivery frequency of 1 Hz because of concern for heart fibrillation. However, in most of our preliminary studies including the first clinical prostate cancer treatment by IRE protocols,[22] we use a 100- millisecond delivery interval time. A main reason for choosing this frequency is that muscle paralyzing drugs are not used for small animals. We have found in our early studies that this higher frequency generates only a mild and single muscle contraction that the animal can easily bear, without muscle paralyzing drugs. Microscopic evaluation of the NTIRE-ablated zone was performed using an H&E assay. We have performed 3 repeats for each experimental condition, and the results shown here are typical to all the repeats.

Experimental Results

Figure 3 shows the histology of the H&E stained thyroid treated with different voltage over distance between the electrodes (from left to right, 1000 V/cm, 2000 V/cm, and 3000 V/cm) with 10 pulses, top row, and 30 pulses, bottom row. In each photograph, the left lobe is the treated lobe, and the right lobe is the control. The extent of follicular damage increases with an increase in electric field magnitude and an increase in number of pulses. This will be more evident in Figures 4–6, which show magnified details. The ablation area for an electric field of 3000

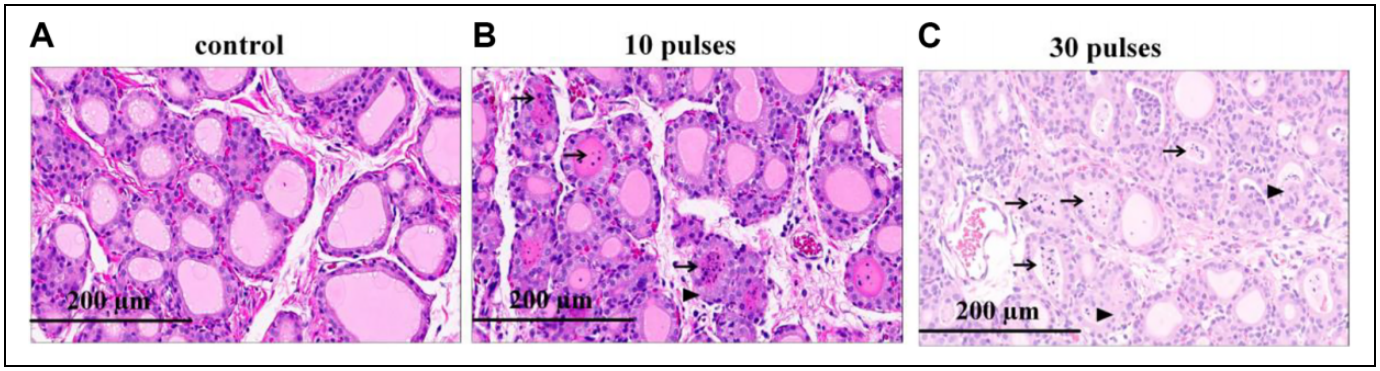

Figure 4. Treatment with voltage/distance of 1000 V/cm. The panels from left are control (A), 10 pulses treated lobe (B), and 30 pulses treated lobe (C). Thin arrows (→) pointed to the colloid filled with infiltrated inflammatory cells and nucleus debris. Triangle arrow (▶) pointed to the follicular cells whose cytoplasmic limits between the cells were barely distinguishable, some nucleus had disappeared.

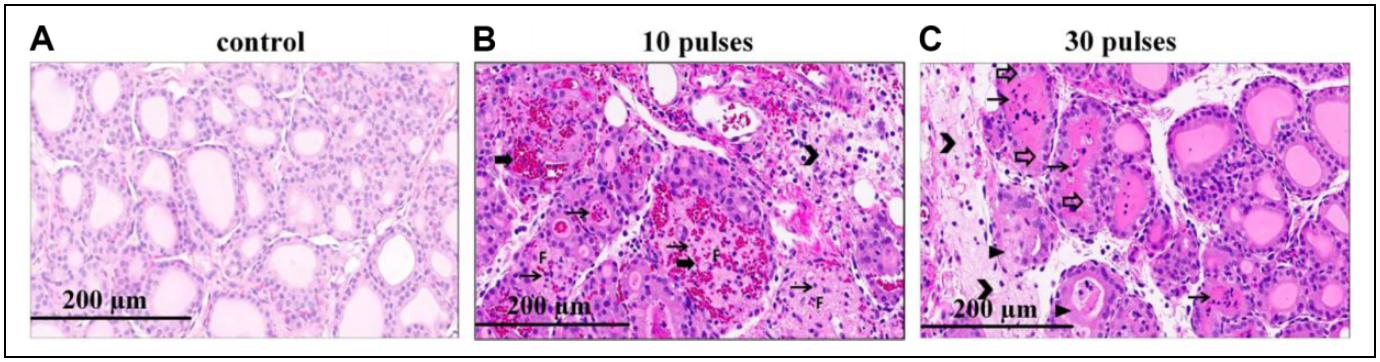

Figure 5. Treatment with 2000 V/cm. The panels from left are control (A), 10 pulses treated lobe (B), and 30 pulses treated lobe (C). Thin arrows (→) pointed to the colloid filled with infiltrated inflammatory cells and nucleus debris. Triangle arrow (▶) pointed to the follicular cells whose cytoplasmic limits between the cells were barely distinguishable, some nucleus had disappeared. Thick arrows (➡) pointed to the congestion and hemorrhagic change in ablation area. The arrow head (❯) pointed to the region of swollen connective tissue. The white arrows (⇨) pointed to the ballooned follicular cells. The letter F represented the follicle, in which the follicular cells had disappeared, nucleus debris, inflammatory cells spread.

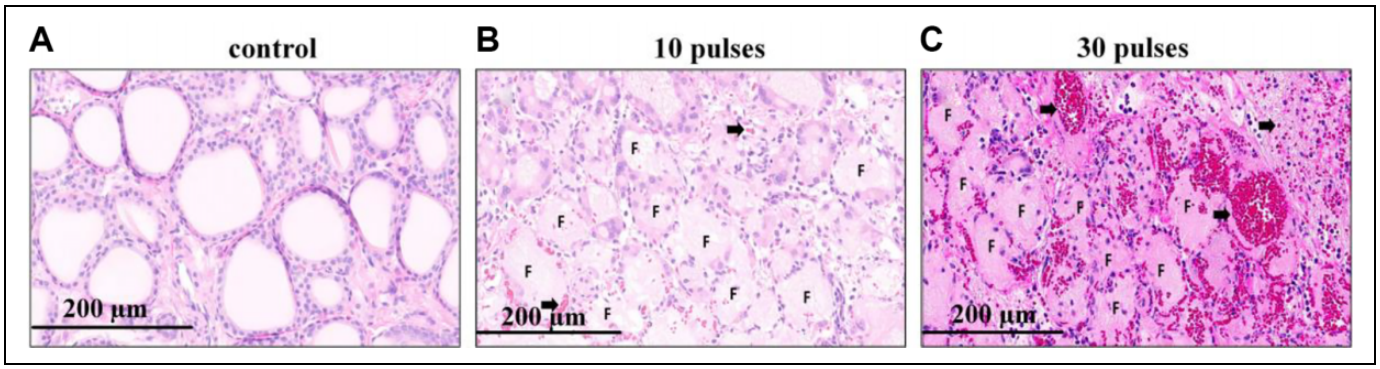

Figure 6. Treatment with voltage/distance of 3000 V/cm. The panels from left are control (A), 10 pulses treated lobe (B), and 30 pulses treated lobe (C). Thick arrows (➡) point to the congestion and hemorrhagic change in ablation area. The letter **F** represents the destroyed follicle, in which the follicular cells had disappeared, nucleus debris, inflammatory cells spread.

V/cm is marked by a dark outline. In that area, most follicular cells have disappeared, and the normal thyroid follicle structure has been destroyed. No change was seen in the control lobes in all samples. Figures 4–6 show magnified details.

Figure 4 shows micrographs of lobes treated with 10 and 30 pulses of voltage/distance 1000 V/cm in comparison with untreated controls, at higher magnification. After treatment, some colloid filled with infiltrated cells and nucleus debris are seen. Some cytoplasmic limits between follicular cells are barely distinguishable. However, most follicle appear intact.

Figure 5 shows higher magnification micrographs of lobes treated with 10 and 30 pulses of voltage/distance of 2000 V/cm

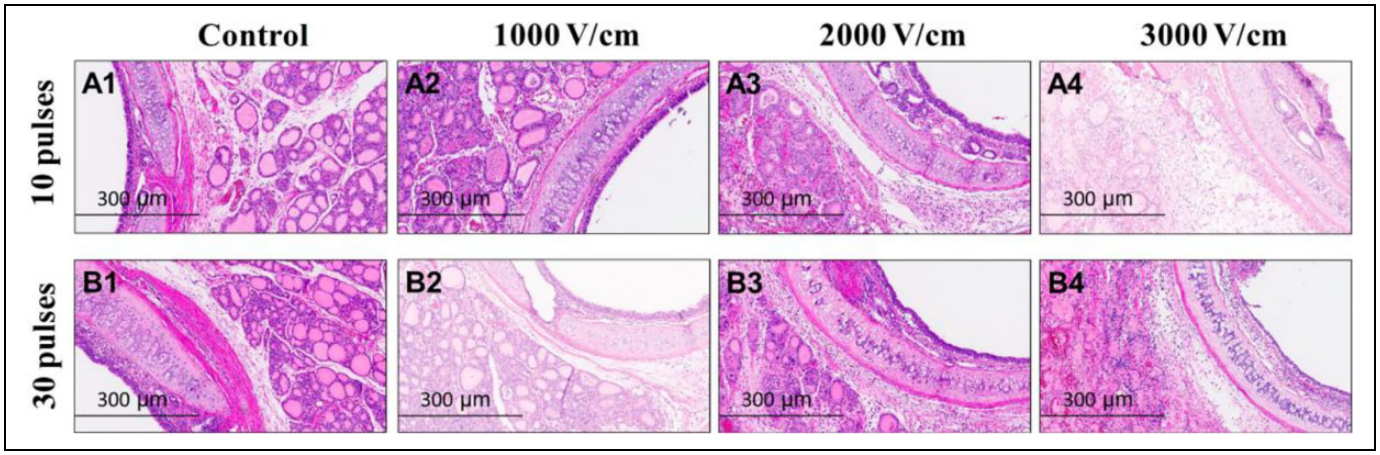

Figure 7. Images at the boundary between the trachea and the thyroid. The upper panels represent 10 pulses treatment, from left are control (A1), 1000 V/cm (A2), 2000 V/cm (A3),and 3000 V/cm (A4). The lower panels represent 30 pulses treatment, from left are control (B1), 1000 V/cm (B2), 2000 V/cm (B3),and 3000 V/cm (B4). Although the follicles were destroyed after the NTIRE treatment, the trachea retains a normal structure. NTIRE indicates nonthermal irreversible electroporation.

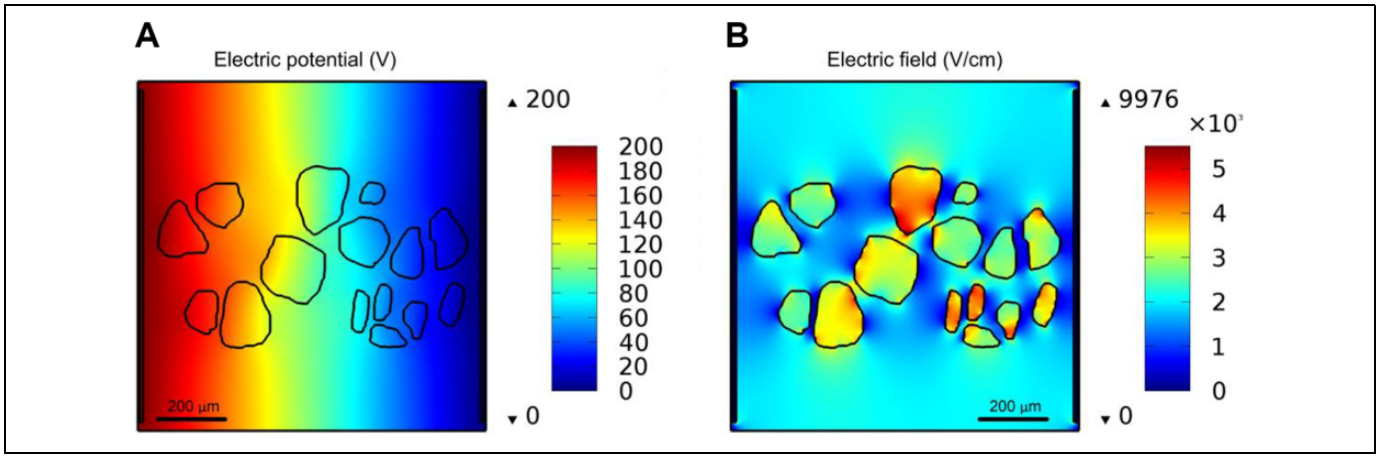

Figure 8. Electric potential distribution (A) and electric field distribution (B) in thyroid tissue. The voltage over distance is 2000 V/cm. The electrode distance is 1 mm.

in comparison with untreated controls. These micrographs show more nuclei debris and inflammatory cells filled with colloid, in comparison to the thyroid tissue treated with 1000 V/cm. Congestion and hemorrhagic changes are also seen in the treated areas. The connective tissue is swollen. Some follicular cells disappeared, and corresponding follicles have lost their normal structure.

Figure 6 shows the changes in the thyroid tissue following treatment with 10 and 30 pulses of voltage/distance 3000 V/cm. The ablation from 3000 V/cm is much more extensive than from 1000 V/cm or 2000 V/cm. Compared to the effects of treatment with 1000 V/cm and 2000 V/cm, after treatment with 3000 V/cm, most follicular cells have disappeared. The ablation is particularly large for 30 pulses. A large amount of thyroid follicles have lost their normal structure. Nucleus debris, inflammatory cells, congestion, and hemorrhagic change are seen throughout the treated area.

Figure 7 shows the morphology of the trachea in controls and near the lobe treated with the different protocols in this study. No difference is seen in the trachea morphology between the part adjacent to the control side and the parts adjacent to the NTIRE treated side, for any of the treatment parameters.

Mathematical Analysis of Electric Fields

Figure 8 illustrates the results of the analysis and shows the electric potential distribution and electric field distribution in the thyroid tissue for the external voltage/distance of 2000 V/cm, between electrodes. Each color band represents a specific voltage range. Figure 8A indicates that the voltage gradient is not uniform in the direction of the applied electric field. Figure 8B demonstrates that the electric field is significantly distorted near the colloidal structures. Moreover, the electric field in the vicinity of the colloid margin is significantly lower than the voltage over distance value of 2000 V/cm. Obviously, the heterogeneity due to the presence of the colloidal structure severely distorts the electric field distribution, thus influencing the thyroid ablation by IRE treatment.

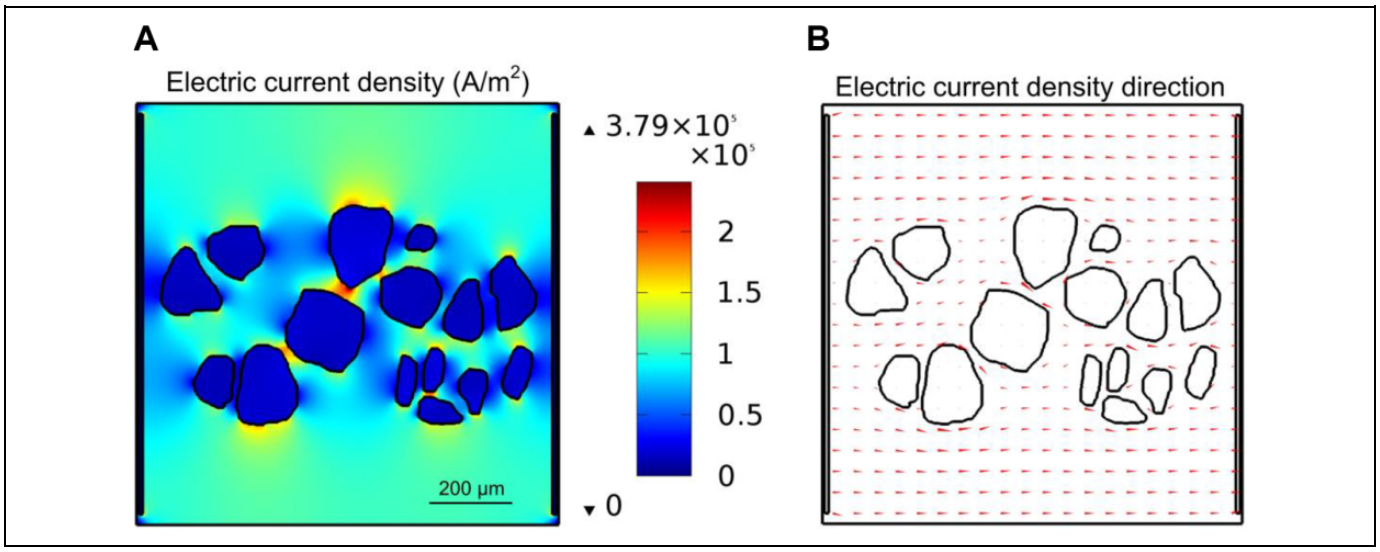

Figure 9. Electric current density distribution (A) and electric current direction arrow (B) in thyroid tissue. The voltage over distance is 2000 V/cm. The electrode distance is 1 mm.

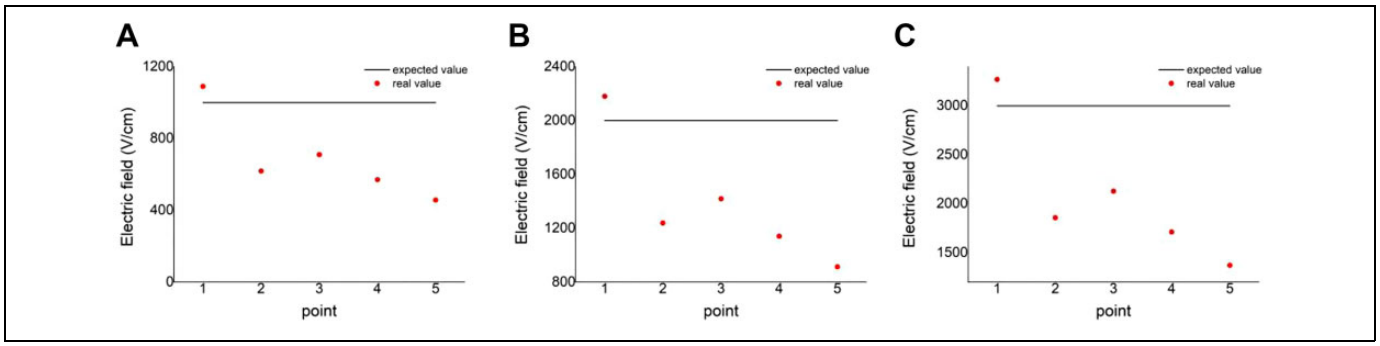

Figure 10. Comparison of the calculated electric field with expected value in homogeneous tissue in the thyroid tissue for 5 different points for the voltage/distance values of 1000 V/cm (A), 2000 V/cm (B), and 3000 V/cm (C).

Figure 9A shows the electric current density distribution in the thyroid tissue and Figure 9B shows the electric current direction in the thyroid tissue. Because of the relatively low conductivity of colloid, the current density is also lower inside the colloid. The electric current density distribution near the circle of colloid was also not uniform. Figure 9B shows the electric current direction arrow in the thyroid tissue. Because of the low conductivity of the colloid relative to the surrounding tissue, the electric current mainly bypasses the colloid and flows around the colloid.

For a more precise analysis, we evaluated the electric field at each of the 5 points marked in Figure 1C for voltage/distance of 1000 V/cm, 2000 V/cm, and 3000 V/cm. The results are displayed in Figure 10. It is interesting to notice that at 4 of the points, the electric field is lower than the respective value of voltage/distance. However, there is also 1 point at which the electric field is higher than the voltage/distance value. For example, the electric field at point 5 is only 903 V/cm, which is 121.5% lower than excepted value of 2000 V/cm. However, the electric field at point 1 is 2180 V/cm, which is 9% higher than the excepted value of 2000 V/cm.

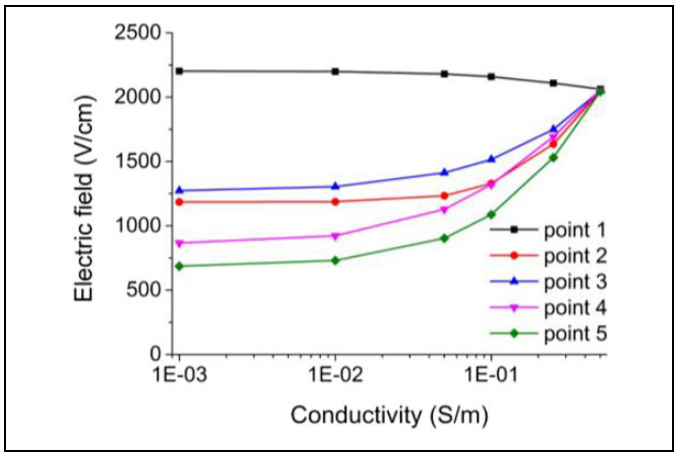

Figure 11. Electric field in the thyroid tissue for 5 different points with increasing conductivity of colloid at the voltage/distance of 2000 V/cm.

Figure 11 shows the electric field in the thyroid tissue for the 5 different points marked in Figure 1C with increasing conductivity of colloid, at the voltage/distance of 2000 V/cm. The

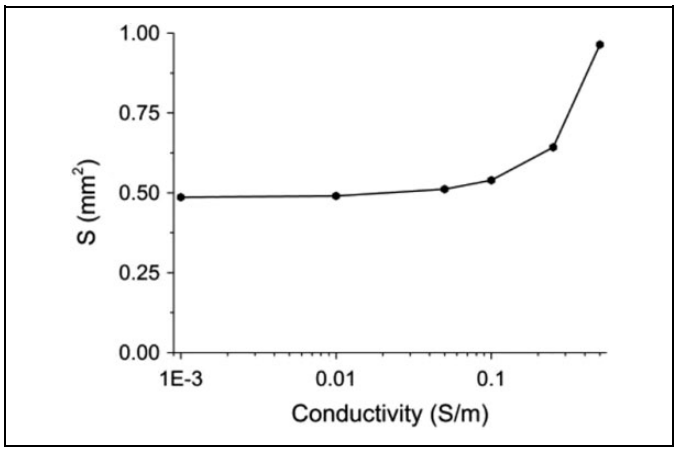

Figure 12. The area S where the local electric field is over the electric field of 2000 V/cm with increasing conductivity of the colloid.

conductivity of thyroid tissue around the colloid was set to be 0.511 S/m. In Figure 10, we show that the electric field at point 1 is higher than the voltage/distance value. Interestingly, with increasing conductivity of the colloid, the electric field at point 5 becomes gradually lower and close to the value of 2000 V/cm. However, at the other 4 points, the electric field increases significantly with increasing conductivity of colloid. When the conductivity of colloid reaches 0.5 S/m, that is, the tissue becomes almost homogeneous, the electric field at all points is close to the value of 2000 V/cm, which is as expected for a homogeneous tissue.

Figure 12 may explain the partial ablation observed with a voltage/distance parameter of 2000 V/cm. It shows the area where the electric field is over the expected value of 2000 V/cm with increasing conductivity of the colloid. The conductivity of thyroid tissue around the colloid was set to 0.511 S/m. It is evident that the area with an electric field close to 2000 V/cm increases when the conductivity of the colloid approaches that of the surrounding tissue. In the nominal conditions, the only half the area around the colloid experiences an electric field of 2000 V/cm. However, when the conductivity of the colloid is 0.5 S/m (close to the conductivity of surrounding thyroid tissue), almost the entire area between the electrodes experiences an electric field of 2000 V/cm, which is as expected in a homogeneous domain. While the mathematical results are obvious, this study describes a real-life configuration. Of practical clinical importance, the heterogeneous nature of the tissue has a critical effect on the treatment with NTIRE.

Mathematical Analysis of Temperature Distribution

To provide an upper limit of the thermal effects, we examined the temperature distribution due to the delivery of a single 1-millisecond long pulse of 3000 V/cm, which is equivalent to 10 pulses of 100 microseconds. The instantaneous upper limit in temperature due to the delivery of this pulse is shown in Figure 13B. There is 1 hot spot at which the temperature is 72.6°C, but the majority of the tissue is at temperatures of 50°C and lower. According to the work of Davalos *et al*,[19] a temperature rise below 50°C is not sufficiently high to cause thermal damage. Figures 13C-E shows that within 1 second, the temperatures drop below 50°C. Since thermal damage is an integration of temperature and time, it is possible to suggest that in this case the damage is mostly nonthermal. Obviously, the heterogeneity of the tissue and the lack of precise thermal data make this analysis tentative.

To provide a further upper limit of the thermal effects, we examined the temperature distribution due to the delivery of a single 3-millisecond long pulse of 3000 V/cm, which is equivalent to 30 pulses of 100 microseconds. The instantaneous upper limit in temperature due to the delivery of this pulse is shown in Figure 14B. There is 1 hot spot at which the temperature is 117°C. However, the majority of the tissue is at temperatures lower than 80°C, and the colloids are at temperatures lower than 50°C. In the temperature range between 80°C and 50°C, the thermal damage is an integration of temperature and

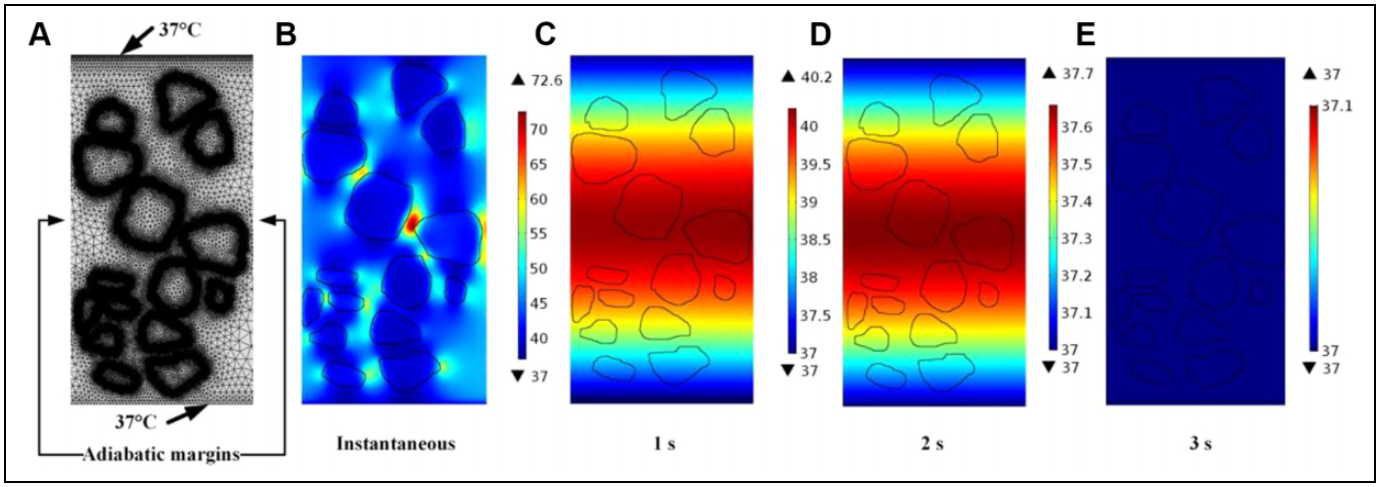

Figure 13. The finite element mesh used in the simulation for thermal analysis (A). The distribution instantaneous (B), 1 (C), 2 (D), and 3 (E) seconds after the treatment by 10 pulses with 300 V.

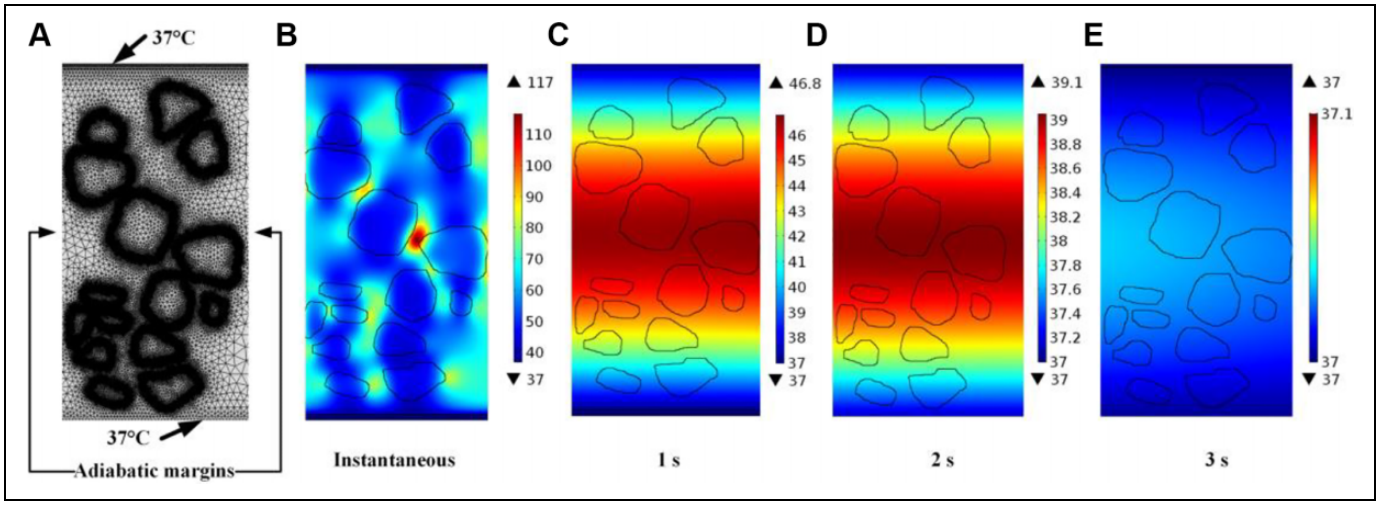

Figure 14. The finite element mesh used in the simulation for thermal analysis (A). The distribution instantaneous (B), 1 (C), 2 (D), and 3 (E) seconds after the treatment by 30 pulses with 300 V.

time. Figures 14 C-E shows that within 1 second, the temperatures drop below the thermal damage threshold.[19] Again a temperature rise below 50°C is not sufficiently high to cause thermal damage.[19] This analysis suggests that while there may be selected sites afflicted by thermal damage, the majority of the treated tissue does not experience thermal damage. Obviously, the heterogeneity of the tissue and the lack of precise thermal data make this analysis tentative. Nevertheless, a possible conclusion is that with 30 pulses of 3000 V/cm, there may be sites in the tissue that experience thermal damage.

Discussion

The primary goals of this study were to introduce the possible use of NTIRE for thyroid tissue ablation and determine (1) whether NTIRE can ablate the thyroid, (2) the effects of various electric field magnitude and number of pulses on the extent of ablation, and (3) the effects of NTIRE treatment of the thyroid on the adjacent trachea.

It should be noticed that the experimental configuration of the thyroid braced between 2 parallel plates appears to generate a 1-dimensional electric field. With this configuration in mind, it was surprising to observe that unusually high electric fields were needed for the tissue ablation. The micrographs in Figure 4 show that for thyroid ablation with 1000 V/cm, there are inflammatory cells and nuclei in the colloid tissue. However, the damage to the follicles is minimal. Most damage happened distal to the trachea. It appears that the extent of damage is similar for a protocol that employed 10 pulses and 30 pulses.

With the voltage increasing to 2000 V/cm, as shown in Figure 5, some follicular cells are swollen, some follicular cells disappeared, and the follicle structure began to disintegrate. The damaged area and the nature of the damage are enhanced relative to treatment with voltage/distance of 1000 V/cm. As with the 1000 V/cm protocol, the increase in number of pulses from 10 to 30 had no effect on the extent of ablation.

Increasing the voltage/distance to 3000 V/cm caused most follicle structure to collapse. The significance of this is that the follicles have lost their secretion of thyroid hormone function, which would have been the goal of the NTIRE treatment. The damaged area occupied almost the whole treated lobe. An interesting observation from the parametric studies is that the extent of ablation is strongly related to the magnitude of the electric field. However, the number of pulses has no noticeable effect. The image J was used to calculate the thyroid ablation region. The ablation area by 10 pulses with 3000 V/cm is 3.18 ± 0.50 mm^2. The ablation area by 30 pulses with 3000 V/cm is 2.75 ± 1.20 mm^2. There is no statistically significance ($P = .599$) between 10 and 30 pulses (analysis of variance method).

In addition to tissue ablation by electroporation, there are several additional mechanisms of damage. They are mechanical damage from the compression of the thyroid, electrolysis from the electrochemical reaction at the electrodes, and thermal from Joule heating. Concerning mechanical damage, the experiments show that there is minimal damage at the low electric fields. Therefore, this suggests that even if the mechanical pressure had an effect, it is minor relative to the effect of the electric fields. Electrolysis is a possible additional mechanism of damage and it could occur simultaneously with electroporation. This was shown in other studies as well. Saulis *et al*[36] and Turjanski *et al*[37] also found that the electrolysis products which are inadvertently generated during any type of electroporation are detrimental in cells and tissues. Rubinsky *et al*[38] found that the NTIRE electric pulses could induce the electrolysis effect which will cause cytotoxic effect for cells during the tissue electroporation. Stehling *et al*[39] also showed that combination of electroporation and electrolysis could be able to ablate the liver tissues. In this study, the NTIRE protocols we used may also induce electrolysis effect, which may be involved in the thyroid ablation. The thermal analysis also provides interesting results. The extreme heterogeneity of the thyroid suggests that there may be hot spots at which there is

thermal damage, at least for the upper limit of the electroporation parameters of 30 pulses of 3000 V/cm. The analysis suggests that the majority of the treated tissue does not experience conditions inducive to thermal damage—however, the lack of precise thermal data of this highly heterogeneous tissue requires caution with this conclusion.

Since the thyroid is very close to the trachea, the effect of NTIRE pulses on the trachea is a key consideration in using NTIRE for the ablation of the thyroid. We monitored the morphology of trachea near the thyroid treated with NTIRE. No changes were seen to the trachea no matter for any of the electric fields and pulse numbers in this study, including those that caused complete ablation of the thyroid.

Several findings emerge from this first feasibility study on the ability to ablate thyroids with NTIRE. First, it is evident that NTIRE is capable of complete follicle ablation in the treated area and the extent of ablation increases with an increase in electric field; 3000 V/cm is an electric field that can yield complete ablation in the treated volume. Second, in all our experiments, the trachea was not affected by NTIRE applied to the thyroid. This suggests that the technique is safe to apply near the trachea. This is consistent with the findings of others. The main reason is that NTIRE affects only the cell membrane and does not affect the connective tissue. In the small intestines, we found that the endothelial cells around the lumen completely regenerate after the NTIRE treatment.[40]

The study of the NTIRE treatment of the thyroid gave us the opportunity to examine mathematically the effects of tissue heterogeneity on the NTIRE treatment in a situation of clinical importance. Most of the fundamental research on NTIRE was done in macroscopically homogeneous and isotropic tissues such as the liver, or the brain or homogeneous and anisotropic tissues such as the muscle. However, the thyroid represents an extreme case of a heterogeneous tissue, with a large difference in electrical conductivity between different macroscopic regions. At first, we were surprised that 3000 V/cm are needed to completely ablate the target region. There are several factors above the electric fields expected to ablate mammalian cells of the type and dimensions in the thyroid. The mathematical model shows that if there are low conductivity macroscopic inclusions in the tissue, the voltage/distance is not a good measure of the electric fields experienced by the treated tissue and careful design is needed for such heterogeneous tissues.

Finally, our study is a first order short-term feasibility study that suggests the potential of the technique. Larger studies and longer follow-ups will be needed before the technique can be considered for clinical treatment. As mentioned earlier, this is a first order study to demonstrate the feasibility and the electrical parameters needed to ablate thyroid tissue. We choose 24 hours as the end point time to evaluate thyroid ablation, because of our past experience from studies with molecular and immunological responses to NTIRE liver tissue ablation. In those studies, we found that necroptosis and pyroptosis are the key mechanisms of cell ablation by NTIRE and these processes cease at 24 hours; after which hepatocytes begin to regenerate. Obviously, the thyroid is different from the liver and substantial more research is needed to understand the dynamics of NTIRE-induced thyroid ablation. Therefore, when considering the clinical use of NTIRE for thyroid ablations, practitioners are cautioned that the research in this field is by no means complete.

Conclusion

The results of this study suggest that NTIRE has the potential to become a minimally invasive technique for thyroid ablation as a possible treatment of hyperthyroidism and thyroid cancer. We found that surprisingly high voltages over distance are needed for thyroid tissue ablation. The mathematical analysis suggests that the high voltage over distance needed is due to the highly heterogeneous structure of the thyroid. A general conclusion emerges from this study, when highly heterogeneous structures are treated with NTIRE, the voltage over distance parameters of electroporation have a very weak relation to the actual electric fields that the tissues experience.

We would like to emphasize that the main goal of this article is to introduce thyroid tissue ablation as a new and possible valuable application of NTIRE. While the results of the experiments are conclusive, the mathematical models used to analyze the results are hampered by the lack of reliable data on the thermal and electrical properties of the highly heterogeneous thyroid tissue. Therefore, the mathematical analysis makes what we consider reasonable first order assumptions on the electrical and thermal properties of the thyroid. However, obviously, more precise studies with better properties data should be done in the future.

Authors' Note

Yanpeng Lv and Yanfang Zhang made equal contributions to this study.

Ethical Statement

All animals received humane care from properly trained professionals in compliance with both the Principals of Laboratory Animal Care and the Guide for the Care and Use of Laboratory Animals, published by the National Institute of Health (NIH publication no. 85-23, revised 1985). The UC Berkeley Animal Care and Use Committee approval is AUP-2017-01-94530.

Declaration of Conflicting Interests

The author(s) declared no potential conflicts of interest with respect to the research, authorship, and/or publication of this article.

Funding

The author(s) disclosed receipt of the following financial support for the research, authorship, and/or publication of this article: the Mechanical Engineering Department at UC Berkeley, China Scholarship Council (CSC), the National Natural Science Foundation of China (No. 081702768), the Henan Province Key Science and Technology Projects (No. 162102310009), and the Luoyang Science and Technology Projects (No. 1603001A-13).

ORCID iD

Yanpeng Lv https://orcid.org/0000-0001-8554-0652

References

1. Policeni BA, Smoker WR, Reede DL. Anatomy and embryology of the thyroid and parathyroid glands. *Semin Ultrasound CT MR*. 2012;33(2):104-114.
2. Inoue K, Couch EF, Takano K, Ogawa S. The structure and function of folliculo-stellate cells in the anterior pituitary gland. *Arch Histol Cytol*. 1999;62(3):205-218.
3. Yen PM. Physiological and molecular basis of thyroid hormone action. *Physiol Rev*. 2001;81(3):1097-1142.
4. Cooper DS. Hyperthyroidism. *Lancet*. 2003;362(9382): 459-468.
5. Boelaert K, Torlinska B, Holder RL, Franklyn JA. Older subjects with hyperthyroidism present with a paucity of symptoms and signs: a large cross-sectional study. *J Clin Endocrinol Metab*. 2010;95(6):2715-2726.
6. Goichot B, Caron P, Landron F, Bouée S. Clinical presentation of hyperthyroidism in a large representative sample of outpatients in France: relationships with age, aetiology and hormonal parameters. *Clin Endocrinol (Oxf)*. 2016;84(3): 445-451.
7. Burch HB, Cooper DS. Management of graves disease: a review. *JAMA*. 2015;314(23):2544-2554.
8. Mohlin E, Nyström Filipsson H, Eliasson M. Long-term prognosis after medical treatment of graves' disease in a northern Swedish population 2000-2010. *Eur J Endocrinol*. 2014;170(3): 419-427.
9. Elbers L, Mourits M, Wiersinga W. Outcome of very long-term treatment with antithyroid drugs in graves' hyperthyroidism associated with graves' orbitopathy. *Thyroid*. 2011;21(3): 279-283.
10. Abraham P, Avenell A, McGeoch SC, Clark LF, Bevan JS. Antithyroid drug regimen for treating graves' hyperthyroidism. *Cochrane Database of Systematic Reviews*. 2010;20(1): CD003420.
11. Nakamura H, Miyauchi A, Miyawaki N, Imagawa J. Analysis of 754 cases of antithyroid drug-induced agranulocytosis over 30 years in japan. *J Clin Endocrinol Metab*. 2013;98(1): 4776-4783.
12. Cooper DS. Antithyroid drugs. *N Engl J Med*. 2005;352(9): 905-917.
13. Burch HB, Burman KD, Cooper DS. A 2011 survey of clinical practice patterns in the management of graves' disease. *J Clin Endocrinol Metab*. 2012;97(12):4549-4558.
14. Bahn RS, Burch HB, Cooper DS, et al. American Thyroid Association, American Association of Clinical Endocrinologists. . Hyperthyroidism and other causes of thyrotoxicosis: management guidelines of the American Thyroid Association and American Association of Clinical Endocrinologists. *Thyroid*. 2011;21(6): 593-646.
15. Pradeep PV, Agarwal A, Baxi M, Agarwal G, Gupta SK, Mishra SK. Safety and efficacy of surgical management of hyperthyroidism: 15-Year experience from a tertiary care center in a developing country. *World J Surg*. 2007;31(2):306-312.
16. Weaver JC, Chizmadzhev YA. Theory of electroporation: a review. *Bioelectrochem Bioenerg*. 1996;41(2):135-160.
17. Rubinsky B. Experimental studies on non-thermal irreversible electroporation in Tissue. In: Rubinsky B, ed. *Irreversible Electroporation. Series in Biomedical Engineering*. Berlin, Heidelberg: Springer; 2010:155-181.
18. Neumann E, Schaeffer-Ridder M, Wang Y, Hofschneider PH. Gene transfer into mouse lymphoma cells by electroporation in high electric fields. *EMBO J*. 1982;1(7):841-845.
19. Davalos RV, Mir LM, Rubinsky B. Tissue ablation with irreversible electroporation. *Ann Biomed Eng*. 2005;33(2): 223-231.
20. Edd JF, Horowitz L, Davalos RV, Mir LM, Rubinsky B. In vivo results of a new focal tissue ablation technique: irreversible electroporation. *IEEE Trans Biomed Eng*. 2006;53(7):1409-1415.
21. Rubinsky B, Onik G, Mikus P. Irreversible electroporation: a new ablation modality - clinical implications. *Technol Cancer Res Treat*. 2007;6(1):37-48.
22. Onik G, Rubinsky B. Irreversible electroporation: first patient experience focal therapy of prostate cancer. In: Rubinsky B, ed. *Irreversible Electroporation. Series in Biomedical Engineering*. Berlin, Heidelberg: Springer; 2010:235-247.
23. Thomson KR, Cheung W, Ellis SJ, et al. Investigation of the safety of irreversible electroporation in humans. *J Vasc Interv Radiol*. 2011;22(5):611-621.
24. Martin RCG, Durham AN, Besselink MG, et al. Irreversible electroporation in locally advanced pancreatic cancer: a call for standardization of energy delivery. *J Surg Oncol*. 2016;114(7): 865-871.
25. Neven K, Van ESR, Van Driel V, et al. Acute and long-term effects of full-power electroporation ablation directly on the porcine esophagus. *Circ Arrhythmia Electrophysiol*. 2017;10(5): e004672.
26. Wittkampf FHM, Van ESR, Neven K. Electroporation and its relevance for cardiac catheter ablation. *JACC Clin Electrophysiol*. 2018;4(8):977-986.
27. Srimathveeravalli G, Wimmer T, Monette S, et al. Feasibility and acute safety following catheter directed IRE for endoluminal ablation of the porcine esophagus. *J Vasc Interv Radiol*. 2014; 25 (3):S31.
28. Burmeister LA, Goumaz MO, Mariash CN, Oppenheimer JH. Levothyroxine dose requirements for thyrotropin suppression in the treatment of differentiated thyroid cancer. *J Clin Endocrinol Metab*. 1992;75(2):344-350.
29. Lin CL, Wu SY, Huang WT, et al. Subsequent thyroid disorders associated with treatment strategy in head and neck cancer patients: a nationwide cohort study. *BMC Cancer*. 2019;19(1): 461.
30. Scheffer HJ, Melenhorst MCAM, Echenique AM, et al. Irreversible electroporation for colorectal liver metastases. *Tech Vasc Interv Radiol*. 2015;18(3):159-169.
31. Tasu J.P, Vesselle G, Herpe G, et al. Tougeron, irreversible electroporation for locally advanced pancreatic cancer: where do we stand in 16 2017? *Pancreas*. 2017;46(3):283-287.

32. Zhang Y, Lyu C, Liu Y, Lv Y, Chang TT, Rubinsky B. Molecular and histological study on the effects of non-thermal irreversible electroporation on the liver. *Biochem Biophys Res Commun*. 2018;500(3):665-670.
33. Kandadai MA, Raymond JL, Shaw GJ. Comparison of electrical conductivities of various brain phantom gels: developing a 'brain gel model'. *Mater Sci Eng C Mater Biol Appl*. 2012;32(8):2664-2667.
34. Gabriel C. Compilation of the Dielectric Properties of Body Tissues at RF and Microwave Frequencies. *Radiofrequency Radiation Division*. San Antonio, TX: Brooks AFB. 1996;AL/OE-TR-1996-0037.
35. Daniels C, Rubinsky B. Electrical field and temperature model of nonthermal irreversible electroporation in heterogeneous tissues. *J Biomech Eng*. 2009;131(7):071006.
36. Saulis G, Lap R, Praneviiūt R, et al. Changes of the solution pH due to exposure by high-voltage electric pulses. *Bioelectrochemistry*. 2005;67(1):101-108.
37. Turjanski P, Olaiz N, Maglietti F, et al. The role of pH fronts in reversible electroporation. *Plos One*. 2011;6(4):e17303.
38. Rubinsky L, Guenther E, Mikus P, et al. Electrolytic effects during tissue ablation by electroporation. technology in cancer research & treatment. 2016;15(5):NP95.
39. Stehling MK, Guenther E, Mikus P, et al. Synergistic combination of electrolysis and electroporation for tissue ablation. *Plos One*. 2016;11(2):e0148317.
40. Phillips M, Narayan R, Padath T, Rubinsky B. Irreversible electroporation on the small intestine. *Br J Cancer*. 2012;106(3):490-495.